The Plant Cell, Vol. 27: 1352–1366, April 2015, www.plantcell.org

Suppression of Arbuscule Degeneration in *Medicago truncatula phosphate transporter4* Mutants Is Dependent on the Ammonium Transporter 2 Family Protein AMT2;3

Florence Breuillin-Sessoms,[a,1,2] Daniela S. Floss,[a,1] S. Karen Gomez,[a,3,4] Nathan Pumplin,[a,3,5] Yi Ding,[a,3] Veronique Levesque-Tremblay,[a] Roslyn D. Noar,[a,6] Dierdra A. Daniels,[a] Armando Bravo,[a] James B. Eaglesham,[a] Vagner A. Benedito,[b,7] Michael K. Udvardi,[b] and Maria J. Harrison[a,8]

[a] Boyce Thompson Institute for Plant Research, Tower Road, Ithaca, New York 14853
[b] Samuel Roberts Noble Foundation, Ardmore, Oklahoma 73401

During arbuscular mycorrhizal (AM) symbiosis, the plant gains access to phosphate (Pi) and nitrogen delivered by its fungal symbiont. Transfer of mineral nutrients occurs at the interface between branched hyphae called arbuscules and root cortical cells. In *Medicago truncatula*, a Pi transporter, PT4, is required for symbiotic Pi transport, and in *pt4*, symbiotic Pi transport fails, arbuscules degenerate prematurely, and the symbiosis is not maintained. Premature arbuscule degeneration (PAD) is suppressed when *pt4* mutants are nitrogen-deprived, possibly the result of compensation by PT8, a second AM-induced Pi transporter. However, PAD is also suppressed in nitrogen-starved *pt4 pt8* double mutants, negating this hypothesis and furthermore indicating that in this condition, neither of these symbiotic Pi transporters is required for symbiosis. In *M. truncatula*, three AMT2 family ammonium transporters are induced during AM symbiosis. To test the hypothesis that suppression of PAD involves AMT2 transporters, we analyzed double and triple Pi and ammonium transporter mutants. *ATM2;3* but not *AMT2;4* was required for suppression of PAD in *pt4*, while *AMT2;4*, but not *AMT2;3*, complemented growth of a yeast ammonium transporter mutant. In summary, arbuscule life span is influenced by PT4 and ATM2;3, and their relative importance varies with the nitrogen status of the plant.

INTRODUCTION

Most vascular flowering plants are capable of forming symbioses with obligate biotrophic fungi of the phylum Glomeromycota, generally referred to as arbuscular mycorrhizal (AM) fungi (Lanfranco and Young, 2012). These mutualistic associations develop in the plant roots where the AM fungi colonize the cortex to access carbon from the plant. In addition, the fungi develop an extraradical mycelium that captures mineral nutrients from the soil. Subsequently, some of these nutrients are transferred to the plant (Smith and Read, 2008).

Phosphorus (P) and nitrogen (N), two major mineral nutrients required by plants, can both be acquired through the symbiosis (reviewed in Smith and Smith, 2011). AM fungi can transfer substantial amounts of P, as phosphate (Pi), to their plant hosts and as Pi is relatively immobile in the soil, this usually has a major impact on plant growth (Sanders and Tinker, 1971). The effects of N delivery through the symbiosis are less apparent, likely because nitrate and ammonium ions are mobile in the soil and therefore more readily accessible to the root. However, tracer studies demonstrate that N transfer between fungal symbionts and their hosts does occur (Johansen et al., 1993; Hodge et al., 2001) and in certain circumstances the quantities can be significant (Tanaka and Yano, 2005; Leigh et al., 2009; Hodge and Fitter, 2010). The symbiosis is also regulated in response to these mineral nutrients, and colonization levels decrease when shoot P or N levels are high (Koide and Li, 1990; Blanke et al., 2005; Breuillin et al., 2010).

During AM symbiosis, mineral nutrients are delivered to the plant through arbuscules, highly branched hyphae that develop in the cortical cells. Arbuscules are surrounded by the periarbuscular membrane, which is continuous with the plasma membrane of the root cell but is 4- to 10-fold larger in surface area; thus, the arbuscule and periarbuscular membrane provide an extensive interface for nutrient exchange (reviewed in Harrison, 2012). Despite their beneficial function, arbuscules are terminally differentiated structures with a relatively short life span and they degenerate after ~4 to 8 d depending on the species involved (Alexander et al., 1988, 1989). In an active symbiosis, development of new arbuscules and degeneration of old arbuscules occur continuously in the root cortex.

Symbiotic P and N transfer begins in the extraradical hyphae where uptake from the soil is followed by long-distance transfer

[1] These authors contributed equally to this work.
[2] Current address: College of Biological Sciences/Biotechnology Institute, University of Minnesota, St. Paul, MN 55108.
[3] These authors contributed equally to this work.
[4] Current address: School of Biological Sciences, University of Northern Colorado, Greeley, CO 80639.
[5] Current address: Department of Biology, Swiss Federal Institute of Technology (ETH-Zurich), 8092 Zurich, Switzerland.
[6] Current address: Department of Plant Pathology, North Carolina State University, Raleigh, NC 27695.
[7] Current address: Plant and Soil Sciences Division, West Virginia University, Morgantown, WV 26506.
[8] Address correspondence to mjh78@cornell.edu.
The author responsible for distribution of materials integral to the findings presented in this article in accordance with the policy described in the Instructions for Authors (www.plantcell.org) is: Maria J. Harrison (mjh78@cornell.edu).
www.plantcell.org/cgi/doi/10.1105/tpc.114.131144

to the arbuscules. The current models suggest that Pi and N move as polyphosphate (polyP) and arginine, respectively, and that translocation through the hyphae occurs in vacuoles (Cox et al., 1980; Govindarajulu et al., 2005; Cruz et al., 2007; Hijikata et al., 2010). In yeast, polyP and arginine are physically associated and a similar suggestion has been made for AM fungi (Durr et al., 1979; Govindarajulu et al., 2005). Once the polyP and arginine reach the arbuscule, they are catabolized. Pi and ammonium are released from the arbuscule to the periarbuscular apoplast where they can be accessed by plant transporters on the periarbuscular membrane (Ezawa et al., 2001; Govindarajulu et al., 2005; Cruz et al., 2007). Currently, transporters or channels involved in these efflux processes are unknown.

Symbiosis-inducible ammonium transporters of the AMT2 family have been identified in several plant species (Gomez et al., 2009; Guether et al., 2009; Kobae et al., 2010; Hong et al., 2012; Ruzicka et al., 2012; Koegel et al., 2013; Pérez-Tienda et al., 2014). The *Lotus japonicus* and sorghum (*Sorghum bicolor*) transporters Lj-AMT2;2, Sb-AMT3;1, and Sb-AMT4 each complement growth of a yeast ammonium transporter mutant, and Lj-*AMT2;2* showed a K_m for ammonium of 0.83 mM when expressed in *Xenopus laevis* oocytes (Guether et al., 2009; Koegel et al., 2013). Two ammonium transporters, soybean (*Glycine max*) AMT4;1, and *S. bicolor* AMT3;1, were localized in the periarbuscular membrane (Kobae et al., 2010; Koegel et al., 2013). Given these data, it seems very likely that these transporters function in ammonium transport across the periarbuscular membrane; however, the existence of multiple paralogs may complicate functional analyses.

Several phosphate transporter genes are induced transcriptionally during symbiosis (reviewed in Karandashov and Bucher, 2005; Harrison et al., 2010; Yang and Paszkowski, 2011), and members of the PHOSPHATE TRANSPORTER1 (PHT1) subfamily 1 have prominent roles in symbiosis (Javot et al., 2007; Yang et al., 2012; Xie et al., 2013). PHT1 subfamily 1 transporters PT4 of *Medicago truncatula*, PT11 of rice (*Oryza sativa*), and PT4 of *Astragalus sinicus* are localized in the periarbuscular membrane (Harrison et al., 2002; Paszkowski et al., 2002; Kobae and Hata, 2010; Xie et al., 2013), and the respective mutants fail to show increases in shoot Pi content or shoot growth during symbiosis (Javot et al., 2007; Yang et al., 2012; Xie et al., 2013). Furthermore, in os-*pt11*, tracer studies confirmed that Pi was not delivered via the fungus during symbiosis (Yang et al., 2012). Loss of transporter function also affected survival of the fungus, and mt-*pt4*, os-*pt11*, and As-*PT4* RNA interference (RNAi) roots each contained a high proportion of degenerate arbuscules (Javot et al., 2007; Yang et al., 2012; Xie et al., 2013). In mt-*pt4*, arbuscule development occurred normally but degeneration was initiated prematurely within 48 h of fungal entry to the root. Premature arbuscule degeneration (PAD) resulted in the failure of the fungus to become established in the root and loss of symbiosis (Javot et al., 2007). These data indicate a causal relationship between loss of transporter function and arbuscule degeneration and support the hypothesis that symbiotic Pi transport is essential for maintenance of the symbiosis.

The mechanism underlying PAD is unknown, and initially it was proposed that PAD might result from a reduction in carbon supply arising from a failure in symbiotic Pi transfer. However, PAD still occurs when *M. truncatula pt4* mutants are colonized by hyphae arising from a productive association with a nurse plant (Javot et al., 2011), which argues against a carbon starvation phenomenon. Although PAD cannot be suppressed with an external carbon supply, it is strongly influenced by the N status of the plant; PAD can be fully suppressed if the *pt4* mutants are starved for N (Javot et al., 2011). Suppression occurs only in response to N starvation and not to S or K starvation (Javot et al., 2011). Here, we continue to investigate the connection between symbiotic nutrient transport, arbuscule life span, and maintenance of AM symbiosis. Analyses of double and triple Pi and ammonium transporter mutants reveal a role for an AMT2 family protein in arbuscule maintenance in *pt4*.

RESULTS

Identification of PT8, a Second AM Symbiosis-Inducible Pi Transporter

The observation that PAD in *pt4* occurs only if the plants are grown with sufficient N was unexpected (Javot et al., 2011). If the hypothesis that symbiotic Pi transport is essential for maintenance of the symbiosis is true, then in *pt4* mutants, another Pi transporter(s) should compensate for PT4 during growth in low N conditions. To identify additional Pi transporters, we performed in silico searches of the *M. truncatula* genome. These revealed a total of 13 Pi transporter genes (Supplemental Figure 1), seven of which (*PT1-PT6* and *PT9*) have been reported previously (Liu et al., 1998, 2008; Chiou et al., 2001; Harrison et al., 2002; Xiao et al., 2006; Grunwald et al., 2009; Floss et al., 2013). The genes that were not reported previously included *PT7*, *PT8*, and *PT10-13* (official nomenclature *MEDtr;Pht1;7*, *MEDtr;Pht1;8*, and *MEDtr;Pht1;10*, *MEDtr;Pht1;11*, *MEDtr;Pht1;12*, and *MEDtr;Pht1;13*). Of these 13 transporter genes, only *PT4* and *PT8* are induced in mycorrhizal roots (Figure 1A). Phylogenetic analysis showed that PT8 is a member of subfamily I and is an ortholog of *A. sinicus* PT1 (Xie et al., 2013) and of soybean Glyma14g36650, which has two names, Gm-PT7 (Tamura et al., 2012) and Gm-PT10 (Qin et al., 2012).

Based on its AM symbiosis-induced expression pattern, PT8 was the most promising candidate for a role in symbiotic Pi transport and was selected for further analysis. Expression of *PT8* in the yeast Pi transport-defective strain PAM2 complemented the growth defect in PAM2, and PAM2/*PT8* showed growth rates comparable to PAM2/*PT4*, suggesting that PT8 functions as a Pi transporter (Figure 1B). When expressed under the control of its native promoter, a PT8-GFP (green fluorescent protein) fusion was detected exclusively in cortical cells harboring arbuscules (Figure 1C; Supplemental Figures 2A and 2B) and localized in the periarbuscular membrane as observed previously for PT4. To evaluate the role of PT8 during AM symbiosis, a *M. truncatula* line harboring a transposon in the *PT8* coding sequence was identified from the *M. truncatula* Tnt1 insertion mutant population. The 5.3-kb retrotransposon was inserted 657 nucleotides downstream of the first ATG (Supplemental Figure 3) and is predicted to result in a truncated protein with only 5 of the 12 membrane spanning domains. Following inoculation with *Glomus intraradices*, colonization levels and arbuscule

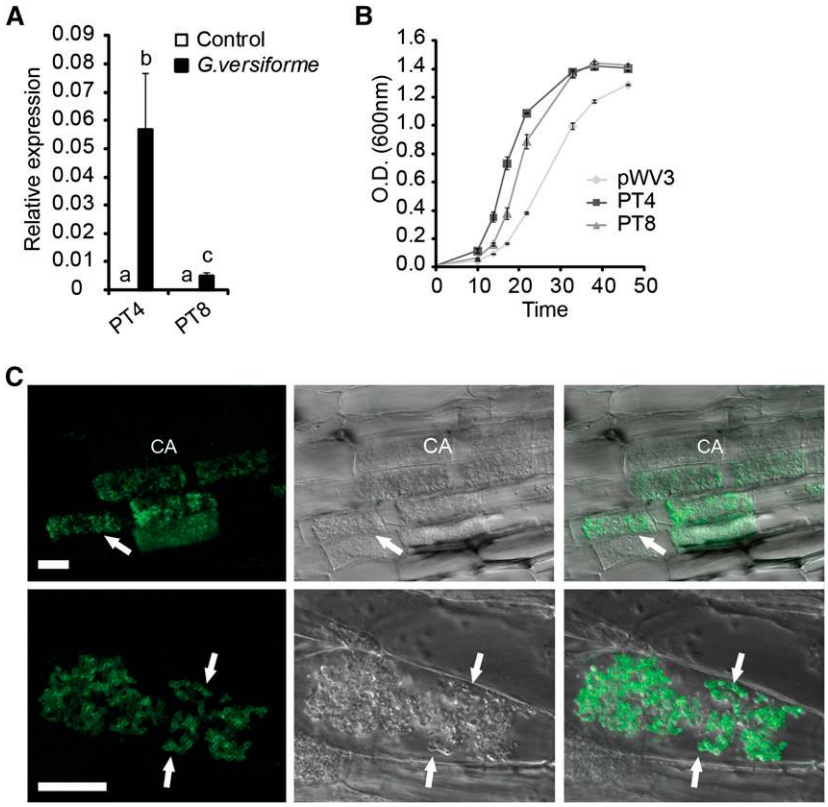

Figure 1. Expression and Localization of PT8.

(A) Quantitative RT-PCR analysis showing the transcript levels of *PT8* and *PT4* relative to *EF1*-α in roots of *M. truncatula* A17 at 5 wpi with *G. versiforme*. Data are the means of three biological replicates ± SE. Different letters indicate significant differences at (α = 0.01).

(B) Growth curves of the yeast phosphate transporter mutant strain PAM2 transformed with an empty vector (pWV3) or *PT4* and *PT8*. The OD of three biological replicates was measured at 0 h, 10 h, 13 h 45 min, 17 h, 21 h 45 min, 32 h 45 min, 38 h, and 48 h.

(C) *M. truncatula* roots expressing $MtPT8_{pro}$*:MtPT8-GFP* colonized with *G. versiforme.* Upper panels: GFP signal from $MtPT8_{pro}$*:MtPT8-GFP* is observed in cells with arbuscules (arrow); the signal is weak or absent in cells with collapsed arbuscules (CA). Lower panels: A single cortical cell harboring an arbuscule displays PT8-GFP signal in the branch domain of the periarbuscular membrane. Left panel, GFP fluorescence obtained by confocal microscopy; middle panel, bright-field differential interference contrast; right panel, overlay. Upper panels, seven 1.22-μm optical sections; lower panels, seven 0.35-μm optical sections. Bars = 20 μm.

morphology in *pt8-1* did not differ from that of the wild type (Supplemental Figures 2C and 2D). Furthermore, arbuscule populations, as assessed by monitoring arbuscule length at 4, 6, and 8 d post-contact with primed spores (Lopez-Meyer and Harrison, 2006), did not differ significantly in *pt8-1* and the wild type, illustrating that arbuscule development and arbuscule life span do not differ in these two lines (Supplemental Figure 2E). Thus, in contrast to PT4, loss of PT8 function does not result in PAD. Consistent with the appearance of a wild-type symbiosis, *pt8-1* plants showed a similar benefit from the AM symbiosis as wild-type plants with an increase in shoot mass and shoot Pi content (Supplemental Figures 2F and 2G).

PT8 Is Not Required for the Suppression of PAD in *pt4* in Low-N Conditions

To determine if PT8 was required for suppression of PAD in *pt4* mutants, we created two independent *pt4 pt8* double mutants. The first double mutant, *pt4-2 pt8-1*, results from a cross between the null allele, *pt4-2* (A17 background), and *pt8-1* (R108 background). The second double mutant, *pt4-5 pt8-1*, results from a cross between a null insertion allele of *PT4*, named *pt4-5* (R108 background) (Supplemental Figure 3) and *pt8-1* (R108 background). The phenotypes of the two double mutants were compared with the respective single mutants and with the two corresponding wild-type parents. When inoculated with *Glomus versiforme*, both of the double Pi transporter mutants displayed mycorrhizal phenotypes not significantly different from that of *pt4*. During growth in conditions with high N, the PAD phenotype, typified by a low percentage of large mature arbuscules and a high percentage of small arbuscules with septa, was apparent in both single *pt4* alleles and in both *pt4 pt8* double mutants (Figures 2A and 2B; Supplemental Figure 4A). During growth in low-N conditions, PAD was suppressed in both *pt4* single mutants and also in the double Pi transporter mutants. The percentages of arbuscules in the 45- to 75-μm size class in

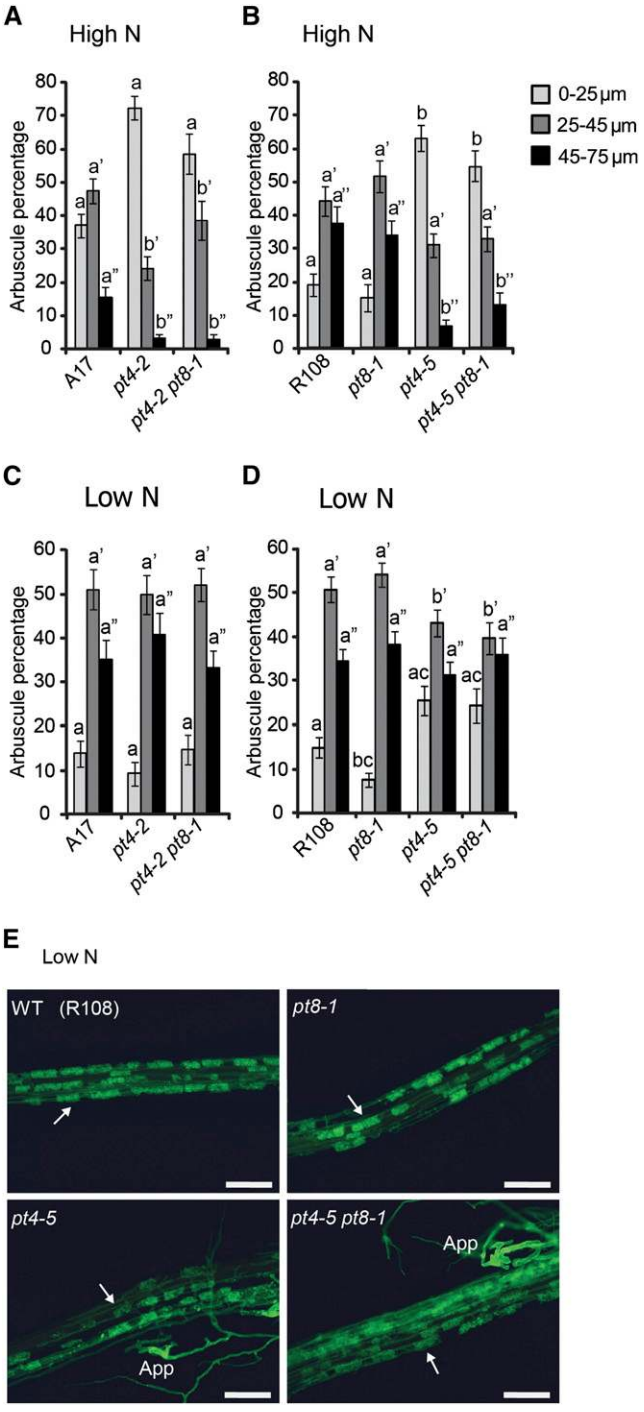

Figure 2. Arbuscule Development in Pi Transporter Single and Double Mutants during Growth in High-N and Low-N Conditions.

(A) Arbuscule size distribution in arbuscule populations in A17 (wild type), *pt4-2*, and *pt4-2 pt8-1* at 4 wpi with *G. versiforme* grown with high-N (15 mM) fertilization. Data represent the mean ± SE of arbuscules from random infection units (IUs) from A17 (67 IUs), *pt4-2* (54 IUs), and *pt4-2 pt8-1* (38 IUs).

(B) Arbuscule size distribution in arbuscule populations in R108 (wild type), *pt8-1 pt4-5*, and *pt4-5 pt8-1* at 4 wpi with *G. versiforme* grown with high-N (15 mM) fertilization. Data represent the mean ± SE of arbuscules from random IUs from R108 (49 IUs), *pt8-1* (49 IUs), *pt4-5* (76 IUs), and *pt4-5 pt8-1* (63 IUs).

(C) Arbuscule size distribution in arbuscule populations in A17 (wild type), *pt4-2*, and *pt4-2 pt8-1* at 4 wpi with *G. versiforme* grown with low-N (1.5 mM) fertilization. Data represent the mean ± SE of arbuscules from random IUs from A17 (61 IUs), *pt4-2* (44 IUs), and *pt4-2 pt8-1* (51 IUs).

(D) Arbuscule size distribution in arbuscule populations in R108 (wild type), *pt8-1*, *pt4-5*, and *pt4-5 pt8-1* at 4 wpi with *G. versiforme* grown with high-N (15 mM) fertilization. Data represent the mean ± SE of arbuscules from random IUs from R108 (83 IUs), *pt8-1* (82 IUs), *pt4-5* (94 IUs), and *pt4-5 pt8-1* (65 IUs).

In **(A)** to **(D)**, different letters indicate significant differences ($\alpha = 0.01$).

(E) Fluorescence microscopy images of *G. versiforme* IUs in R108 (wild type), *pt8-1*, *pt4-5*, and *pt4-5 pt8-1* at 4 wpi grown with low-N (1.5 mM) fertilization. Arrows indicate mature arbuscules. App indicates appressorium. Bars = 100 µm.

the single *pt4* mutants and double Pi transporter mutants were not significantly different from those in *pt8-1* or in the wild-type parents (Figures 2C to 2E). Minor differences in the proportion of arbuscules in the small and mid-size arbuscule classes were observed in *pt4-5* and *pt4-5 pt8-1* double mutant but not in *pt4-2* or the *pt4-2 pt8-1* double mutant (Figures 2C and 2D). This may result from differences in timing for full suppression of PAD in the two ecotypes, likely resulting from differences in their responses to nutrient deprivation. The R108 ecotype shows symptoms of P and N starvation more readily than A17 and accumulates less Pi than the A17 ecotype. Because of the differential mineral nutrient sensitivity, the conditions to achieve N deprivation in the two ecotypes were slightly different (see Methods). In both ecotypes, low-N conditions led to higher shoot P levels (Supplemental Tables 1 and 2), which is consistent with the suppressive effect of N on shoot Pi accumulation reported for *Arabidopsis thaliana* (Kant et al., 2011). In both high-N and low-N conditions, the N content of the double mutants tended to be higher than the single mutants or wild-type plants. Otherwise, with respect to shoot weight and P content, the double mutants did not differ from the respective single mutants or their wild-type parents.

PAD and low-N suppression of PAD were also observed following colonization of the mutant with *G. intraradices* (Supplemental Figure 4B). Overall, the data indicate that the PAD phenotype in *pt4* grown in high-N conditions is independent of PT8; furthermore, PT8 function is not required for suppression of PAD in low-N conditions. Current analyses suggest that PT4 and PT8 are the only Pi transporters present in the periarbuscular membrane in *M. truncatula* (Liu et al., 2008). Consequently, it appears that symbiotic Pi transport across the periarbuscular membrane is not required for arbuscule survival when the plants have a low-N status.

Suppression of PAD in *pt4* Mutants Requires AMT2 Family Protein, AMT2;3 but Not AMT2;4

Given our findings that suppression of PAD occurs only in N-deprived *pt4* and does not require PT8, we considered the possibility that symbiotic N transfer was required for suppression of PAD in *pt4*. The current data suggest that ammonium is

the form of N transferred from the fungus to the plant (Govindarajulu et al., 2005; Cruz et al., 2007), and in several plants species, ammonium transporters of the AMT2 family are induced during AM symbiosis and are located in the peri-arbuscular membrane (Gomez et al., 2009; Guether et al., 2009; Kobae et al., 2010; Koegel et al., 2013). In *M. truncatula*, we identified six genes in the AMT2 family, four of which were reported recently (Straub et al., 2014); therefore, we follow their nomenclature. Our phylogenetic analysis revealed two distinct clades in the AMT2 family, the first clade contains *AMT2;3*,

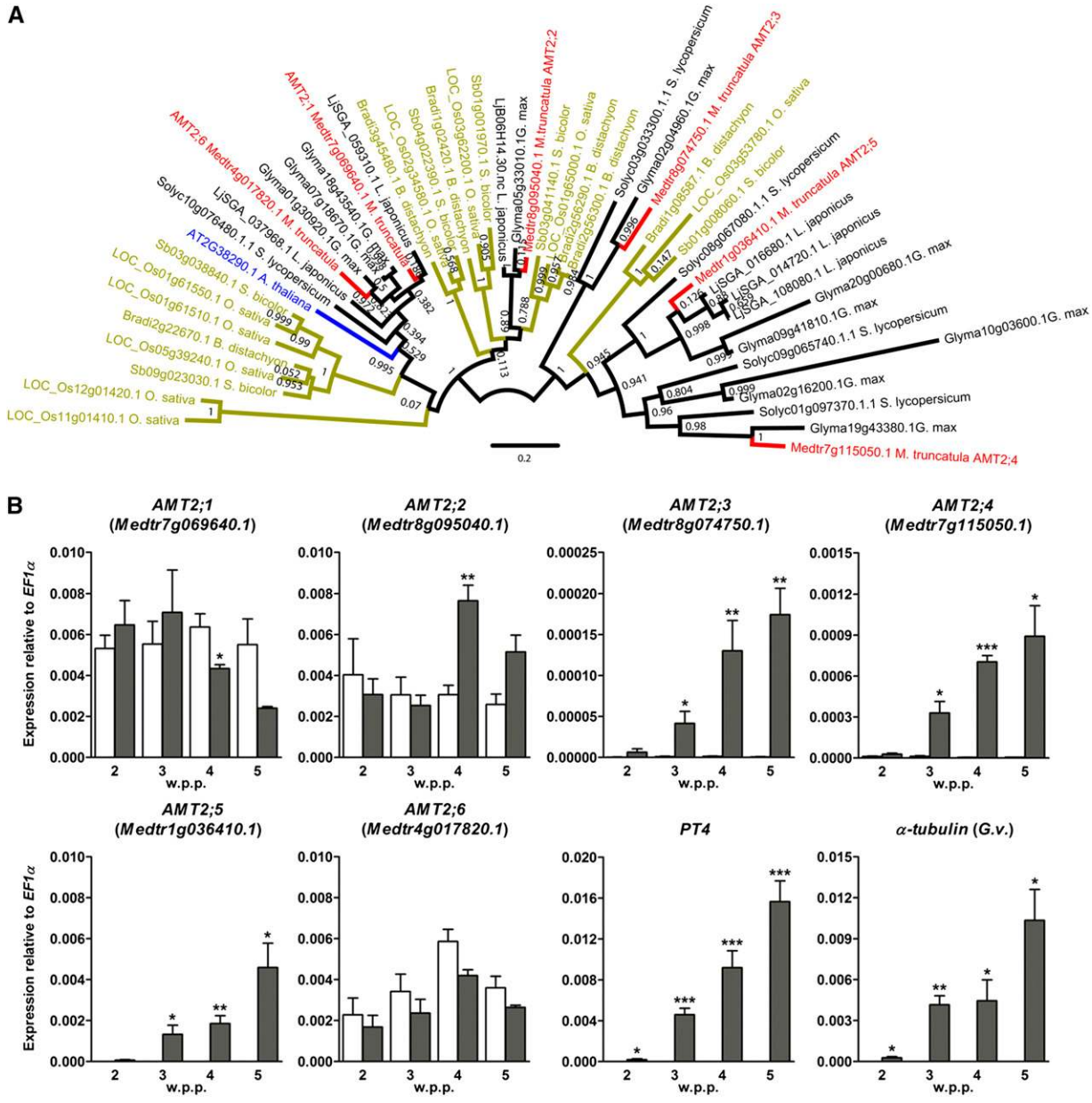

Figure 3. Phylogeny of the *M. truncatula* AMT2 Family and Expression during AM Symbiosis.

(A) The approximately maximum likelihood phylogenetic tree was generated using the predicted full-length amino acid sequences of AMT2 transporters from Arabidopsis, tomato (*Solanum lycopersicum*), rice, sorghum, *L. japonicus*, soybean, and *M. truncatula*. Each branch division shows local support values with the Shimodaira-Hasegawa test (Price et al., 2010).

(B) Transcript levels of *AMT2;1* to *AMT2;6* genes in A17 roots either mock-inoculated (white bars) or colonized by *G. versiforme* (gray bars) at 2, 3, 4, and 5 wpp assayed by quantitative RT-PCR. Transcript levels of *G. versiforme* α-*tubulin* and *PT4* provide an indication of the colonization level and arbuscule abundance respectively. Data are averages ± SE ($n \geq 3$ where n denotes the number of independent root samples). Significant differences (Student's t test) between *G. versiforme* colonized roots and corresponding mock-inoculated control samples are indicated (*P ≤ 0.05, **P ≤ 0.01, and ***P ≤ 0.001). For AMT2;1, the 5 wpp control sample, $n = 2$ and, therefore, statistical analyses were not conducted for this sample.

AMT2;4, and *AMT2;5*, while the second contains *AMT2;1*, *AMT2;2*, and *AMT2;6* (Figure 3A). The single Arabidopsis *AMT2* gene clusters with the second clade. *AMT2;3*, *AMT2;4*, and *AMT2;5* transcripts are low or absent in noncolonized roots and increase significantly during AM symbiosis. In all three cases, transcript levels correlate with colonization and arbuscule levels as assessed by *G. versiforme* α-tubulin and *PT4* transcript levels, respectively (Figure 3B). However, the relative abundance of the individual *AMT2* transcripts differs substantially. For example, *AMT2;3* transcripts are 30-fold less abundant than *AMT2;5* transcripts (Figure 3B). In contrast, members of the second clade, *AMT2;1*, *AMT2;2*, and *AMT2;6*, are constitutively expressed and their transcripts are relatively abundant and do not change substantially during symbiosis. Previously, we showed that *AMT2;3* transcripts were present in cells with arbuscules (Gomez et al., 2009); consequently, we focused initially on this member of the AMT2 family. To extend this initial analysis, we examined the expression patterns and location of the AMT2;3 protein. Surprisingly, noncolonized *M. truncatula* roots expressing an *AMT2;3* promoter-GFP fusion construct showed GFP fluorescence in the cortex and endodermis (Figure 4A), although transcripts were barely detected in roots prior to symbiosis (Figure 3B). Following colonization, GFP fluorescence was restricted to cells containing arbuscules, which suggests changes in promoter activity during symbiosis (Figure 4B).

To examine the location of the AMT2;3 protein, N-terminal and C-terminal *AMT2;3-GFP* fusions expressed from the *AMT2;3* promoter were analyzed. In both cases, we did not detect GFP fluorescence in control roots; however, Straub et al. (2014) reported weak, diffuse fluorescence from an AMT2;3-GFP fusion in control roots. In colonized roots, our analyses revealed that the GFP signal was extremely weak and was either associated with the arbuscule branches (Figure 4C) or visible as a diffuse haze (Figure 4D). Based on these data and the fact that other symbiosis-induced AMT2 family proteins have been localized to the periarbuscular membrane (Kobae et al., 2010; Koegel et al., 2013), we make a tentative conclusion that AMT2;3 is located in the periarbuscular membrane. The relatively high frequency of cells showing a diffuse, hazy signal suggests that the protein fusions are relatively unstable. Whether this is an inherent property of AMT2;3 or an effect of the GFP fusion is unclear. Stability issues were not reported for the AMT2-GFP fusions studied previously in soybean (Kobae et al., 2010; Koegel et al., 2013).

A *M. truncatula* line with a Tnt1 insertion positioned 465 bp downstream of the first ATG of the *AMT2;3* gene was obtained from the *M. truncatula* Tnt1 insertion mutant population (Supplemental Figure 3). This insertion truncates the protein at amino acid 155, resulting in a protein with less than four transmembrane domains. The mutant was backcrossed to R108, and the mycorrhizal phenotype was evaluated in the BC1F3 generation. There were no apparent differences in the morphology of the symbiosis in *amt2;3* roots relative to the R108 wild-type parent or to a wild-type segregant plant selected from the backcrossed *amt2;3* F2 population. The number of infection units and numbers of arbuscules in *amt2;3* and R108 roots were assessed during growth at three levels of N fertilization and no significant differences were observed (Table 1). Additionally, the

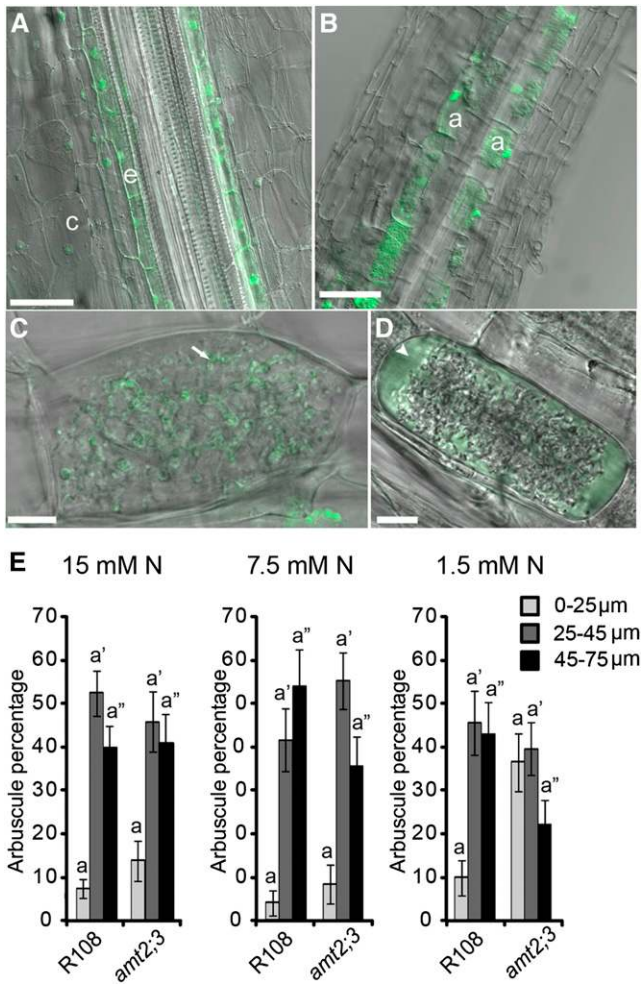

Figure 4. *AMT2;3* Expression, Localization of AMT2;3-GFP, and Arbuscule Populations in *amt2;3*.

(A) and **(B)** *M. truncatula* roots expressing *AMT2;3*$_{pro}$:*GFP*. Control roots **(A)** and roots colonized with *G. versiforme* **(B)**. Images are single optical sections and show GFP fluorescence overlayed on the corresponding differential interference contrast image. Cortex (c), endodermis (e), and cells containing arbuscules (a). Bars = 100 µm.

(C) and **(D)** Single cells from *M. truncatula* roots expressing *AMT2;3*$_{pro}$:*AMT2;3-GFP* and *AMT2;3* $_{pro}$:*GFP-AMT2;3* colonized with *G. versiforme*. Images are single optical sections and show GFP fluorescence overlayed on the corresponding differential interference contrast image. Arrow points to fluorescence associated with an arbuscule branch. Arrowhead points to fluorescence associated with the vacuole. The fluorescence patterns obtained with the two constructs did not differ significantly. Bars = 10 µm.

(E) Arbuscule size distribution in arbuscule populations in R108 (wild type) and *amt2;3* at 4 wpi with *G. versiforme* grown with 15 mM (FS1), 7.5 mM (FS2), and 1.5 mM (FS3) N fertilization. Data represent the mean ± SE of arbuscules from random infection units from R108 (28 IUs) and *amt2;3* (26 IUs) at 15 mM N, R108 (12 IUs) and *amt2;3* (25 IUs) at 7.5 mM N, and R108 (28 IUs) and *amt2;3* (33 IUs) at 1.5 mM N. Different letters indicate significant differences (α = 0.01).

Table 1. Colonization of *amt2;3* during Growth with Differing Levels of N Fertilization

N Treatment	Genotype	No. of IUs (3 wpi)	No. of IUs (4 wpi)	No. of Arbuscules per Unit Area (3 wpi)	No. of Arbuscules per Unit Area (4 wpi)
15 mM	R108	20.33 ± 2.33[a]	68.00 ± 9.54[a]	5.22 ± 0.46[a]	4.39 ± 0.48[a]
	amt2;3	22.33 ± 3.93[a]	27.00 ± 3.51[a]	4.16 ± 0.46[a]	3.85 ± 0.46[a]
7.5 mM	R108	14.00 ± 2.65[a']	37.67 ± 9.24[a']	5.10 ± 0.54[a']	4.67 ± 0.48[a']
	amt2;3	20.00 ± 2.65[a']	31.00 ± 2.00[a']	4.92 ± 0.62[a']	4.84 ± 0.58[a']
1.5 mM	R108	25.00 ± 3.06[a'']	30.67 ± 5.84[a'']	6.87 ± 0.64[a'']	3.93 ± 0.49[a'']
	amt2;3	28.33 ± 2.33[a'']	31.67 ± 3.28[a'']	3.73 ± 0.60[b'']	3.52 ± 0.37[a'']

Infection unit number in R108 (wild type) and *amt2;3* at 3 and 4 wpi with *G. versiforme* during fertilization with 15 mM N (FS1), 7.5 mM N (FS2), or 1.5 mM N (FS3) fertilizers. Data represent the mean ± SE of three independent replicates. Different letters indicate significant differences between genotypes for a given treatment or parameter ($\alpha = 0.01$).

structure of the arbuscule populations in *amt2;3* did not differ from those in R108, and there was no evidence of a PAD phenotype in *amt2;3* (Figure 4E; Supplemental Figures 5A to 5C) even in low N, high Pi conditions (Supplemental Figure 5D).

From crosses of *amt2;3* with *pt4-2* and with *pt4-5 pt8-1*, we obtained two independent Pi transporters, ammonium transporter double mutants, *pt4-2 amt2;3* and *pt4-5 amt2;3*, and a triple mutant, *pt4-5 pt8-1 amt2;3*. When grown in high-N conditions, the *pt4-2 amt2;3* and *pt4-5 amt2;3* double mutants and the Pi transporter single mutants *pt4-2* and *pt4-5* colonized with *G. versiforme* all showed PAD (Figures 5A and 5B; Supplemental Figure 6 and Supplemental Table 3), while arbuscule populations in the *amt2;3* single mutant did not differ from those in the wild type. Consequently, we conclude that in high-N conditions, the *pt4* PAD phenotype is independent of *amt2;3*. Surprisingly, during growth in low-N conditions, both double mutants also showed a typical PAD phenotype and the arbuscule populations differed significantly from those in the *pt4* mutants, the *amt2;3* mutant, and both wild-type lines (Figures 5C, 5D, and 5F; Supplemental Figure 7 and Supplemental Table 4). Thus, in low-N conditions, suppression of PAD in *pt4* mutants is dependent on AMT2;3. Furthermore, analysis of the *pt4-5 pt8-1 amt2;3* triple mutant further supports this conclusion; in low-N growth conditions, PAD was not suppressed in the triple mutant (Figure 5E; Supplemental Figure 8 and Supplemental Tables 5 to 7). Under the conditions of these experiments, there were no consistent differences in the shoot mass, shoot phosphorus content, and shoot N content of the wild type, single, and double mutant plants within the low- and high-N conditions (Supplemental Table 4). However in low-N conditions, infection unit length in the triple mutants was lower than that of the respective wild-type control, which is consistent with the PAD phenotype (Supplemental Table 7). Together, these data demonstrate that AMT2;3 function is required for arbuscule survival in *pt4* mutants during growth in low-N conditions. These results were somewhat surprising given that AMT2;3 is one of three closely related *AMT2* genes induced during symbiosis and that *AMT2;3* transcript levels are significantly less abundant than those of *AMT2;4* or *AMT2;5*. Insertions mutants in *AMT2;5* were unavailable, but we were able to obtain an insertion mutant in *AMT2;4*. The transposon is inserted in the first exon after nucleotide 388 and is predicted to result in loss of function (Supplemental Figure 3). As observed for *amt2;3*, the *amt2;4* mutant did not show any apparent defects in AM symbiosis, and its arbuscule population structure was similar to the wild type (Figure 6A). To establish whether AMT2;4 function influenced PAD or suppression of PAD, we generated a *pt4-5 amt2;4* double mutant. In high N conditions, *pt4-5 amt2;4* shows a typical PAD phenotype (Figure 6A), and in low-N conditions, PAD is suppressed as in the *pt4-5* mutant (Figure 6B). These results were confirmed in an additional experiment in which both the *pt4-5 amt2;3* and *pt4-5 amt2;4* double mutants were grown in parallel (Supplemental Figure 9). Consequently, AMT2;3 but not AMT2;4 is required for arbuscule survival in *pt4* in low-N conditions. This unexpected result prompted us to test the ability of *AMT2;3* and *AMT2;4* to complement growth of a yeast high-affinity ammonium transporter mutant strain, 31019b, referred to as the triple *mep* strain (Marini et al., 1997). This strain has been used to evaluate the ammonium transport activities of several plant AMT proteins (Straub et al., 2014), including symbiosis-induced ammonium transporters (Guether et al., 2009; Koegel et al., 2013) as well as fungal transporters such as *G. intraradices* (Gint)-AMT1 (López-Pedrosa et al., 2006). *AMT2;3* and *AMT2;4* were cloned into pYEUra3 under control of the GAL1 promoter, and as expected, triple *mep* transformants carrying the pYEUra3 empty vector, pYEUra3-*MtAMT2;3*, and pYEUra3-*MtAMT2;4* all showed growth on medium containing 5 mM ammonium sulfate with galactose as a carbon source. However, only *AMT2;4* complemented growth of the triple *mep* strain in low-N conditions with either 2 or 0.5 mM ammonium sulfate and galactose as a carbon source (Figure 7). To evaluate protein accumulation in yeast, we introduced *GFP-MtAMT2;3* and *GFP-AMT2;4* fusions into the triple *mep* stain; however, in both cases, the transformants showed only background autofluorescence and the fusion proteins were not detectable (Supplemental Figure 10). Analysis of *AMT2;3* and *AMT2;4* transcripts in the respective *mep* mutant transformants confirmed that both genes were expressed (Supplemental Figure 10).

DISCUSSION

Pi influences the AM symbiosis at multiple levels from regulation of the initial signaling to establishment, maintenance, and functioning of the symbiosis. Furthermore, there are both local and systemic effects; the nutritional status of the plant and the surrounding environment, as well as Pi delivered through the symbiosis, all have an impact on symbiotic development but the underlying mechanisms are mostly unknown (Koide and Schreiner, 1992; Breuillin et al., 2010; Hammer et al., 2011; Kiers et al., 2011; Kretzschmar et al., 2012; Yoneyama et al., 2012).

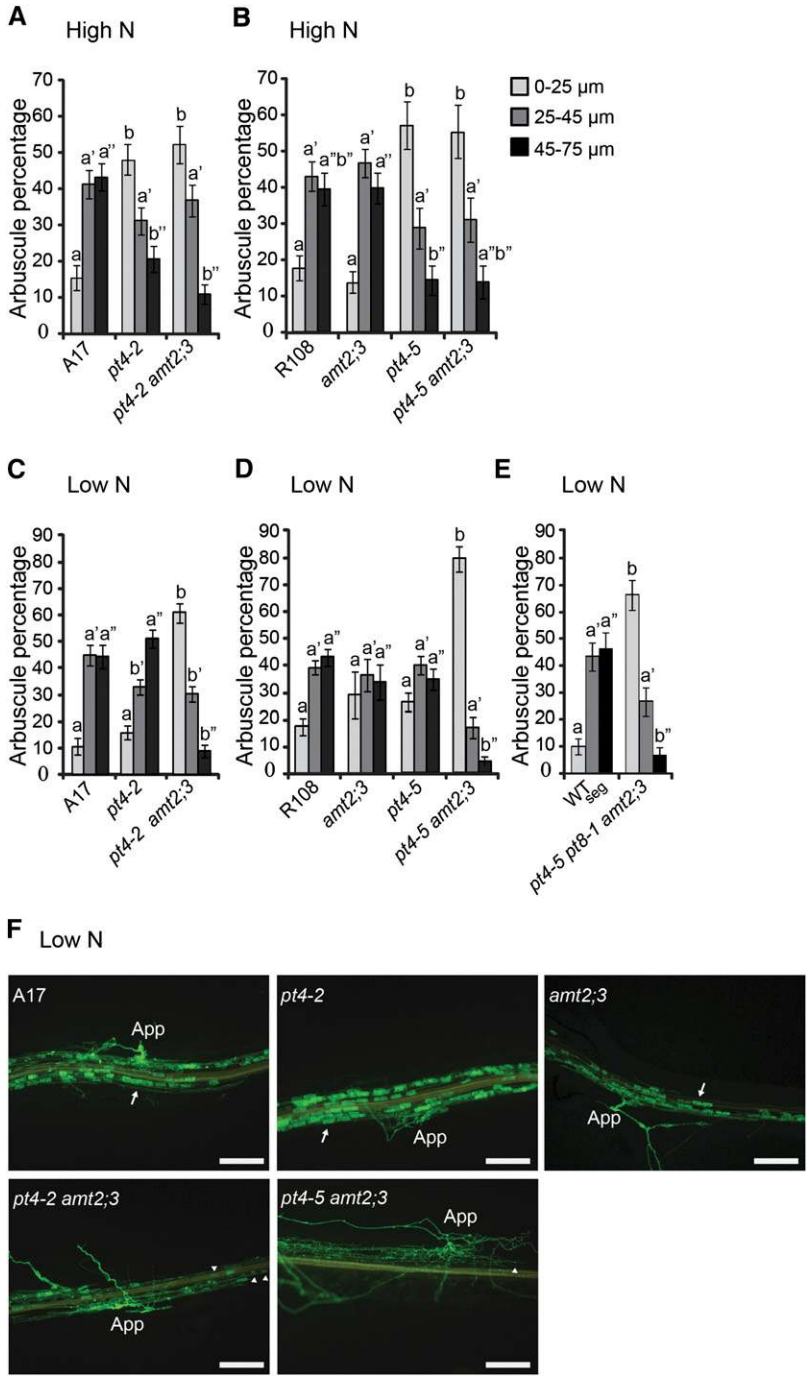

Figure 5. Arbuscule Development in *pt4-5* and *amt2;3* Single, Double, and Triple Mutants during Growth in High-N and Low-N Conditions.

(A) Arbuscule size distribution in arbuscule populations in A17 (wild type), *pt4-2*, and *pt4-2 amt2;3* at 4 wpi with *G. versiforme* grown with high-N (15 mM) fertilization. Data represent the mean ± SE of arbuscules from random IUs from A17 (76 IUs), *pt4-2* (78 IUs), and *pt4-2 amt2;3* (45 IUs).

(B) Arbuscule size distribution in arbuscule populations in R108 (wild type), *amt2;3*, *pt4-5*, and *pt4-5 amt2;3* at 4 wpi with *G. versiforme* grown with high-N (15 mM) fertilization. Data represent the mean ± SE of arbuscules from random IUs from R108 (65 IUs), *amt2;3* (63 IUs), *pt4-5* (34 IUs), and *pt4-5 amt2;3* (26 IUs).

(C) Arbuscule size distribution in arbuscule populations in A17 (wild type), *pt4-2*, and *pt4-2 amt2;3* at 4 wpi with *G. versiforme* grown with low-N (1.5 mM) fertilization. Data represent the mean ± SE of arbuscules from random IUs from A17 (60 IUs), *pt4-2* (86 IUs), and *pt4-2 amt2;3* (80 IUs).

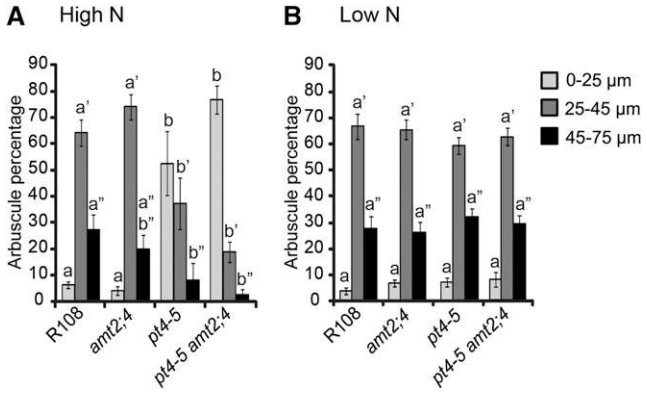

Figure 6. Arbuscule Development in *pt4-5* and *amt2;4* Single and Double Mutants during Growth in High-N and Low-N Conditions.

(A) Arbuscule size distribution in arbuscule populations in R108 (wild type), *amt2;4 pt4-5*, and *pt4-5 amt2;4* at 5 wpi with *G. versiforme* grown with high-N (15 mM) fertilization. Data represent the mean ± SE of arbuscules from random IUs from R108 (14 IUs), *amt2;4* (14 IUs), *pt4-5* (9 IUs), and *pt4-5 amt2;4* (12 IUs).

(B) Arbuscule size distribution in arbuscule populations in R108 (wild type), *amt2;4*, *pt4-5*, and *pt4-5 amt2;4* at 5 wpi with *G. versiforme* grown with low-N (1.5 mM) fertilization. Data represent the mean ± SE of arbuscules from random IUs from R108 (21 IUs), *amt2;4* (19 IUs), *pt4-5* (17 IUs), and *pt4-5 amt2;4* (29 IUs). Different letters indicate significant differences ($\alpha = 0.01$).

Here, we focused on transporters active in the periarbuscular membrane and the influence of their function on arbuscule survival and maintenance of symbiosis.

With the availability of genome sequences and transcriptomes, it has become clear that plants possess at least two PHT1 family Pi transporters whose transcription is increased, sometimes substantially, during AM symbiosis. Furthermore, evolution of symbiosis-regulated Pi transporters has occurred differently among the plant families and variation in the subfamily and in the numbers of symbiosis-regulated transporters is apparent (reviewed in Harrison et al., 2010; Yang and Paszkowski, 2011). Here, we identify PT8, a second Pi transporter induced during AM symbiosis. Like PT4, PT8 shows Pi transport activity when assayed in yeast and the protein is located in the periarbuscular membrane. PT8 is an ortholog of *A. sinicus* PT1 and of soybean Glyma14g36650, which has two names, Gm-PT7 (Tamura et al., 2012) and Gm-PT10 (Qin et al., 2012). Both *A. sinicus* PT1 and soybean Glyma14g36650 are induced during AM symbiosis (Qin et al., 2012; Tamura et al., 2012; Xie et al., 2013). RNAi-mediated downregulation of *PT1* in *A. sinicus* resulted in an alteration in AM symbiosis with a high proportion of small degenerate arbuscules (Xie et al., 2013). In contrast, we found that *pt8* developed symbioses that did not differ from the wild type in fungal colonization levels, arbuscule morphology, symbiotic Pi accumulation, or growth responses. The difference in phenotype of mt-*pt8* and As-*PT1* RNAi roots is surprising and suggests that differences in function have arisen even between closely related transporters.

Although *pt8* did not show an altered AM symbiosis phenotype, we hypothesized that PT8 function might be required for low-N suppression of PAD in *pt4* mutants; however, analysis of *pt4 pt8* double mutants indicated that PAD and low-N suppression of PAD are independent of PT8. Currently, the role of PT8 is unclear. Possibly the most striking finding from Pi transporter double mutants is that despite the importance of Pi in the symbiosis, it appears that symbiotic Pi transporters are not necessary for AM symbiosis in *M. truncatula* if the plants are grown in low-N conditions. In this growth condition, development and maintenance of symbiosis in the double Pi transporter mutant are phenotypically indistinguishable from the wild type grown under the same conditions. As noted previously, under these low-N conditions, wild-type plants do not show an obvious symbiotic growth response likely because N is limiting (Javot et al., 2011). To try to understand the mechanistic basis of these observations, we proposed a model in which Pi delivered to the root cortical cell acts, either directly or indirectly, as a signal that leads to a permissive cellular condition that enables arbuscule survival. The nature of the permissive cellular condition is currently unclear, but two possibilities are carbon release to the fungus or suppression of defenses. There are many examples of rapid cellular changes triggered by mineral nutrients or their primary assimilation products, so the model is not unprecedented (Crawford, 1995; Stitt, 1999; Krouk et al., 2010). Given the suppression of PAD by low-N conditions and the lack of requirement for PT8, we hypothesize that under low-N conditions, N transferred to the cell through the symbiosis also acts as a signal to induce appropriate cellular conditions for arbuscule survival. There is growing evidence for crosstalk between P and N signaling, although currently the underlying mechanisms are unknown (Scheible et al., 2004; Morcuende et al., 2007; Kant et al., 2011). Furthermore, nutritional analysis of AM symbioses suggests that exchange of the most limiting nutrient is maximized (Blanke et al., 2005; Johnson et al., 2010) and reciprocal effects of Pi or N availability on access to carbon have been observed (Kiers et al., 2011; Fellbaum et al., 2012), both of which support aspects of the model. To test aspects of the model, we started to disrupt the putative symbiotic

Figure 5. (continued).

(D) Arbuscule size distribution in arbuscule populations in R108 (wild type), *amt2;3*, *pt4-5*, and *pt4-5 amt2;3* at 4 wpi with *G. versiforme* grown with low-N (1.5 mM) fertilization. Data represent the mean ± SE of arbuscules from random IUs from R108 (82 IUs), *amt2;3* (22 IUs), *pt4-5* (60 IUs), and *pt4-5 amt2;3* (28 IUs). Different letters indicate significant differences ($\alpha = 0.02$).

(E) Arbuscule size distribution in arbuscule populations in a wild-type segregant from the triple mutant population (WTseg) and *pt4-5 pt8-1 amt2;3* at 4 wpi with *G. versiforme* grown with low-N (1.5 mM) fertilization. Data represent the mean ± SE of arbuscules from random IUs WTseg (29 IUs) and *pt4-5 pt8-1 amt2;3* (32 IUs). In **(A)** to **(C)** and **(E)**, different letters indicate significant differences ($\alpha = 0.01$).

(F) Fluorescence microscopy images of *G. versiforme* infection units in A17 (wild type), *pt4-2*, *amt2;3*, *pt4-2 amt2;3*, and *pt4-5 amt2;3* at 4 wpi with low-N (1.5 mM) fertilization. Arrows indicate mature arbuscules. Arrowheads indicate degenerate arbuscules. App indicates appressorium. Bars = 100 µm.

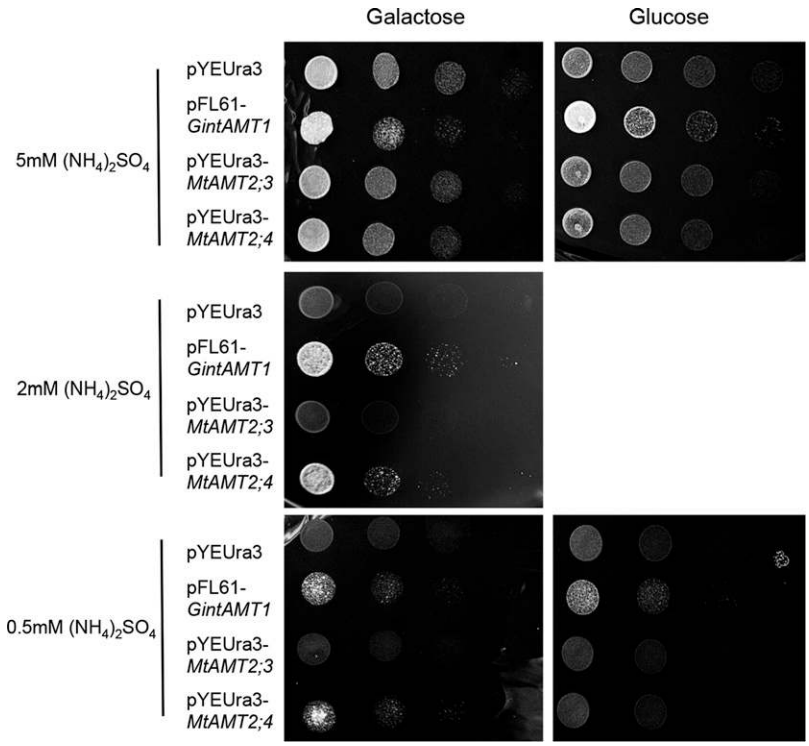

Figure 7. Complementation of a Yeast Ammonium Transporter Mutant by AMT2;4 but Not AMT2;3.

Growth of the yeast 31019b (Δmep1; Δmep2; Δmep3) ammonium transporter triple mutant transformed with pYEUra3 (empty vector), pFL61-*GintAMT1* (López-Pedrosa et al., 2006), pYEUra3-*MtAMT2;3*, and pYEUra3-*MtAMT2;4* on YNB medium containing 5 mM $(NH_4)_2SO_4$, 2 mM $(NH_4)_2SO_4$, or 0.5 mM $(NH_4)_2SO_4$ at pH 4.5 with either glucose or galactose as a carbon source. pFL61-*GintAMT1* serves as a positive control, and expression of Gint-*AMT1* is constitutive (López-Pedrosa et al., 2006). In pYEUra3, the *AMT2;3* and *AMT2;4* genes are expressed from the GAL1 promoter.

ammonium transporters in the background of the *pt4* mutants beginning with AMT2;3 (Gomez et al., 2009).

Mt-*AMT2;3* is predicted to be an ortholog of *G. max AMT4;4*, and both genes are induced during symbiosis (Gomez et al., 2009; Kobae et al., 2010). Surprisingly, the Mt-*AMT2;3* promoter was highly active in cortical cells of noncolonized roots. This was unexpected as *AMT2;3* transcripts were barely detected prior to symbiosis. However, Straub et al. (2014) showed recently that an AMT2;3-GFP fusion protein could be detected at very low levels in control roots, suggesting that the protein is expressed. During symbiosis, AMT2;3-GFP fusion proteins were detected only in cells with arbuscules, and we provide initial evidence that AMT2;3 is located in the periarbuscular membrane as reported for two other symbiosis-inducible AMT2 family proteins, Gm-AMT4;1 and Sb-AMT3;1 (Kobae et al., 2010; Koegel et al., 2013). A similar finding was reported for *S. bicolor*; Sb-AMT3;1 transcripts were detected in cortical cells from noncolonized roots and in noncolonized cortical cells from mycorrhizal roots, but the protein was detected only in cells with arbuscules (Koegel et al., 2013).

We were unable to detect differences in arbuscule development or degeneration, or shoot N and P content in *amt2;3* relative to its wild-type segregant control. However, AMT2;3 function is required for the low-N suppression of the PAD phenotype in *pt4* and *pt4 pt8* mutants. The shoot N content of the *pt4 amt2;3* double and *pt4 pt8 amt2;3* triple mutants was similar to that of the single mutants, which suggests that a failure to suppress PAD is probably not the result of a major change in symbiotic N transport, although a minor change cannot be ruled out. Measuring symbiotic N flow in these double and triple mutants is not feasible because of the severity of the PAD phenotype, which prevents robust development of an extraradical mycelium. Considering our original model, it could be envisaged that low-N suppression of PAD requires a particular level of symbiotic N transfer to the plant and removal of any single AMT2 transporter could potentially reduce symbiotic N flow sufficiently to prevent signaling. However, the finding that a second AM-inducible ammonium transporter, AMT2;4, is not required for PAD argues against this. Alternatively, AMT2;3 may have a specific sensing/signaling function not present in the other AMT transporters. When we tested the ability of AMT2;3 and AMT2;4 to complement a yeast high-affinity transport mutant, only AMT2;4 was able to complement growth in low N media. This suggests that AMT2;3 may have different activities from AMT2;4, although it is also possible that AMT2;3 is unable to function in yeast.

In yeast, the MEP/AMT transporter family contains several carriers that are referred to as transceptors because they sense as well as transport their substrates (Van Nuland et al., 2006; Rubio-Texeira et al., 2010). Similar observations have been made recently in plants. For example, in Arabidopsis, ammonium-induced

lateral root branching is stimulated by a local ammonium supply and the effect is not correlated with overall ammonium uptake, suggesting that it is triggered by ammonium sensing rather than nutritional status. The effect is dependent on only one of the six ammonium transporters, AMT1;3 (Lima et al., 2010). Furthermore, in yeast, MEP2 activates signaling in N-starved cells through the protein kinase A pathway, which is also activated by PHO84 transceptor when Pi is resupplied to Pi-starved cells (Giots et al., 2003; Van Nuland et al., 2006). Consequently, we speculate that transport of Pi or ammonium through the respective symbiotic transporters acts not only to deliver nutrients to the root cell but also initiates signaling that enables conditions for maintenance of arbuscules. Furthermore, signaling involves only a subset of the transporter proteins. In this model, the nutritional status of the plant would determine whether symbiotic delivery of P or N would trigger signaling; this would provide flexibility for regulation of symbiosis during growth in conditions of varying fertility such as those seen in natural ecosystems. A direct role for the transporters in the signaling process is currently speculative but provides a framework for future experiments. Analysis of other *pt4* ammonium transporter double mutants will help to determine whether suppression of PAD is the result of N nutrition or signaling.

METHODS

Medicago truncatula Mutants

In this study, two different subspecies of *M. truncatula* were used, *M. truncatula* ssp *truncatula* ecotype Jemalong (A17) and *M. truncatula* ssp *tricycla* (R108). The *pt4-2* mutant allele described previously (Javot et al., 2007, 2011) is in the A17 background. The *pt4-5*, *pt8*, *amt2;3*, and *amt2;4* alleles are all in the R108 background and are Tnt1 insertion alleles (Supplemental Figure 3) generated at the Noble Foundation or by Pascal Ratet (CNRS, France). The numbers of the *M. truncatula* Tnt1 lines are as follows: NF5213 (*pt8-1*), NF3229 (*amt2;3*), NF4575 (*amt2;4*), and TNK222 (*pt4-5*). The positions of the Tnt1 insertions in the *M. truncatula* lines are shown in Supplemental Figure 3. The primers used to genotype these lines are shown in Supplemental Table 8. All mutant lines were backcrossed to their respective parents. The following double mutants were generated by crossing the respective single mutants: *pt8-1 pt-4-5*, *pt4-2 pt8-1*, *pt4-2 amt2;3*, and *pt4-5 amt2;4*. A *pt4-5 pt8-1 amt2;3* triple mutant was generated by crossing *mtp4-5 mtpt8-1* with *mtamt2;3.* A wild-type segregant from this population was included as a control in the triple mutant analyses.

Plant Growth Conditions

Plants were grown in sterile Turface (calcined clay). At 15 d old, plants were inoculated with surface-sterilized spores of *Glomus versiforme* or *Glomus intraradices*, or mock-inoculated as described previously (Javot et al., 2007, 2011). Briefly, plants were transplanted to new pots or cones that were filled approximately two-thirds full with Turface. The Turface was covered with a 1-cm layer of fine sand. Plants were placed into the pots (or cones) with their roots on the sand, and surface-sterilized spores were pipetted directly onto the roots. The roots were covered with additional Turface, and the plants were maintained in a growth chamber with a 16-h-light (25°C)/8-h-dark (22°C) regime and were fertilized with a modified half-strength Hoagland solution containing 20 μM potassium phosphate unless otherwise described. In the double and triple mutant experiments, plants were inoculated with 300 spores of *G. intraradices* or 600 spores of *G. versiforme*. In pot experiments, each genotype had two pots each containing four plants. In cone experiments, each genotype had three cones each containing two plants. In "double cone" experiments (Lopez-Meyer and Harrison, 2006; Javot et al., 2007), each genotype possessed at least three biological replicates.

For the *M. truncatula*/*G. versiforme* time course (Figure 3), A17 seedlings were planted into cones containing a 1:1 mixture of gravel:sand with a layer of fine sand and 150 surface-sterilized *G. versiforme* spores positioned ~6 cm below the top of the cone. Cones were fertilized twice weekly with half-strength Hoagland solution containing 100 μM potassium phosphate beginning 1 week after planting. Plants were harvested at 2, 3, 4, and 5 weeks post-planting (wpp), and the region of the root system 1 cm above and 1 cm below the sand/spore layer was harvested and frozen for RNA. A small sample was stained to view colonization. Cones harvested at 2 and 3 wpp contained five plants per cone. Cones harvested at 4 and 5 wpp contained four plants per cone. Mock-inoculated control cones received the last washing water from the *G. versiforme* surface sterilization procedure.

Nutrient Treatments

The high-N and low-N fertilizers were FS1, FS2, and FS3 as described previously (Javot et al., 2011). Prior to inoculation, all plants received FS2 fertilizer. After transplanting and inoculation, differential fertilizer treatments were applied beginning 1 week postinoculation (wpi). Fertilizers were applied twice weekly. Genotypes with an A17 background received FS1 (high-N treatment) or FS3 (low-N treatment) twice weekly for 3 weeks. Genotypes with an R108 background received FS2 for 1 week followed by either FS1 for 2 to 3 weeks (high-N treatment) or FS3 for 2 to 3 weeks (low-N treatment). Plants were harvested 4 to 5 wpi.

The double cone experiments were performed as described (Lopez-Meyer and Harrison, 2006; Javot et al., 2007) with the following modifications. Prior to contact between roots and spores, plants received FS2, twice weekly. Following contact between the roots and primed spores, plants received either FS3 solution (low-N condition) or FS1 (high-N condition). Plants were harvested 9 to 12 d post-contact with the spores.

Analysis of Colonization Parameters

Root colonization was assessed using the gridline intersect method and expressed as percentage of root length colonized (McGonigle et al., 1990). For analysis of *amt2;3*, the total number of infection units in the root systems was counted (data shown in Table 1).

Arbuscule size distribution in the arbuscule populations was estimated as described previously with minor modifications (Javot et al., 2011). Briefly, roots were stained with WGA-Alexafluor 488, and infection units were selected at random. One end of each infection unit was imaged at different planes (to capture images of all arbuscule) through the root using a 40× dry objective on a Leica DM5500 epifluorescence microscope, and images were captured using a Retiga 2000R color CCD camera. Images were delimited by the last arbuscule present at the end of the infection unit. The length of each arbuscule was measured using QCapture Pro 6.0 software. For measurements of infection unit length, random infection units were visualized with an Olympus SZX-12 stereomicroscope and images captured with a CCD camera. Infection unit length was then measured using ImageJ software.

Statistical Analysis

For the colonization levels, infection unit size, and arbuscule number and shoot weight, data shown are the means ± SE. The data were tested using JMP software to verify the assumption that they follow a normal distribution. Then, multiple *t* tests were performed between the genotypes within a given treatment (Table 1; Supplemental Tables 1 to 7). The total P and total N data are means ± SD because the individual plants were pooled into two replicates of four plants for these analyses.

For analyses of arbuscule populations, arbuscules were placed into size classes based on their lengths and the percentage of arbuscules in each size class was calculated. Size classes were guided by previous analyses (Javot et al., 2007, 2011). For each class, the average and the SE are graphed. Statistical analyses were conducted on the raw data, and differences between the genotypes were analyzed using a Generalized Linear Model with a Poisson distribution and a log link. The analysis was followed by contrasts to compare the genotypes within each arbuscule size class. A Bonferroni correction was used to adjust the P values for multiple comparisons (Figures 2A to 2D, 4E, 5A to 5E, and 6; Supplemental Figures 2E, 4B, 5D, 7, 8A, 8B. and 9).

Phosphorous and N Shoot Content

Shoot samples from a single pot (four plants) or single cone (two plants) were pooled, oven-dried for 2 d in a 70°C oven, and ground to a fine powder. The N content of the dried shoot powder was measured at the Cornell University Stable Isotope Laboratory (http://www.cobsil.com/index.php) where the samples were analyzed on an elemental analyzer (Carlo Erba NC2500). Total phosphorous content was determined by a phosphomolybdate colorimetric assay (Ames, 1966).

RNA Extraction, cDNA Synthesis, and Quantitative RT-PCR

Total RNA was extracted from root tissues using TRI reagent (Invitrogen) and treated with RNase-free TurboDNaseI (Ambion) followed by a chloroform purification step. First-strand cDNA was synthesized from 1 μg DNase-treated RNA using SuperScript III reverse transcriptase (Invitrogen) in a 20-μL reaction according to the protocol outlined by Gomez et al. (2009). For quantitative RT-PCR, transcripts were amplified from 2 μL of 10× diluted cDNA in a 10-μL reaction using 0.3 μM of each gene-specific primer (Supplemental Table 8) and SYBR Green PCR master mix in an ABI PRISM 7900 HT sequence detection system (Applied Biosystems). Quantitative RT-PCR was performed in 384-well plates with the following PCR cycling conditions: 50°C for 2 min, 95°C for 10 min, 40 cycles of 95°C for 30 s, 58°C for 30 s, and 72°C for 30 s, and a subsequent standard dissociation protocol to exclude primers generating nonspecific PCR products. The threshold cycle (CT) values were calculated using the automatic CT function available with the SDS 2.4 software (Applied Biosystems) and were normalized to the CT values of the housekeeping gene Mt-*EF1*α ($\Delta CT = CT_{Mt\text{-}EF1\alpha} - CT_{gene}$). Relative expression values were calculated ($2^{\Delta CT}$) and were averaged over at least three biological replicates.

Vector Construction

UidA reporter fusions were created in a modified version of the pCAMBIA2301 vector. The *UidA* coding sequence was amplified by PCR with a forward primer adding either a 5′ *Pst*I or 5′ *Hind*III restriction site and a reverse primer that included an endogenous *Best*EII site. The pCAMBIA2301 vector was digested with *Bst*EII and either *Pst*I or *Hind*III, releasing 35S:UidA, and the amplified fragment containing UidA but no promoter was ligated in its place. A genomic fragment encompassing 1139 nucleotides upstream of the PT8 ATG was amplified with primers adding 5′ *Bam*HI and 3′ *Pst*I restriction sites and cloned into the modified 5′ PstI:UidA vector creating *MtPT8*$_{pro}$*:UidA*. The *MtPT8* $_{pro}$*:MtPT8-GFP* translational fusion vector was constructed in the background of a modified pCAMBIA2301 vector containing the S65T GFP variant (Chiu et al., 1996) in the multiple cloning site under control of the cauliflower mosaic virus 35S promoter and NOS terminator. A 2810-bp genomic fragment was amplified from *M. truncatula* A17 DNA corresponding to 1139 bp of sequence upstream of the PT8 ATG and the predicted open reading frame, excluding the stop codon, with primers that add flanking *Bam*HI restriction enzyme sites. The modified pCAMBIA2301 GFP vector was digested with *Bam*HI, which released the 35S promoter. *Bam*HI digestion of the amplified PT8 genomic fragment and ligation into the prepared vector resulted in an in-frame fusion of the 3′ of MtPT8 to the 5′ ATG of GFP. All vectors were sequenced to confirm correct insertions and the absence of introduced mutations.

To create the *AMT2;3* promoter GFP fusion, a 2-kb fragment 5′ of the *AMT2;3* coding sequence was amplified and inserted between the *Age*I and *Nco*I sites in pSAT6-AFP-C1 (1398). The resulting promoter-GFP construct with terminator was then excised with *Age*I and *Not*I, recessed ends were filled in, and the fragment was inserted into *Sma*I-digested pCambia 2301. The C-terminal *AMT2;3*-GFP fusion was created by inserting a 4-kb fragment comprising the *AMT2;3* 5′ flanking sequence and *AMT2;3* gene without the TAA termination codon (2262 bp) between the *Age*I and *Sal*I sites of pSAT6-AFP-N1 (1564). The resulting C-terminal fusion was excised with *Age*I and *Not*I, recessed ends were filled in, and the fragment was inserted into *Sma*I-digested pCambia 2301. The N-terminal GFP-*AMT2;3* fusion was created by adding the *AMT2;3* cDNA (1446 bp) into the *AMT2;3* promoter GFP fusion construct. The *AMT2;3* open reading frame was amplified and inserted between the *Sac*I and *Sal*I sites of pSAT6-AFP-C1 (1398) already containing the *AMT2;3* promoter GFP fusion. The resulting N-terminal fusion was excised with *Age*I and *Not*I, recessed ends were filled in, and the fragment was inserted into *Sma*I-digested pCambia 2301.

Vectors were introduced into *M. truncatula* roots by *Agrobacterium rhizogenes* transformation as described previously (Boisson-Dernier et al., 2001; Pumplin et al., 2010).

Cloning and Complementation of PAM2, a Yeast Phosphate Transport-Defective Strain, with PT8

For analysis of phosphate transport activity in yeast, the PT8 coding sequence was inserted into the yeast expression vector, pWV3 (Versaw and Harrison, 2002) between the *Eco*RI and *Bam*HI sites and transformed into the yeast double phosphate transporter mutant, PAM2 (Martinez and Persson, 1998). Growth of PAM2 expressing PT8 was compared with strains expressing PT4 (Harrison et al., 2002) and an empty vector control.

Cloning of *AMT2;3* and *AMT2;4* into pYEUra3 and Complementation of the Yeast Triple Ammonium Transporter Mutant Strain 31019b

To generate pYEUra3-*MtAMT2;3* and pYEUra3-*MtAMT2;4*, the coding regions of *AMT2;3* (1446 bp) and *AMT2;4* (1443 bp) were amplified with the corresponding primers (Supplemental Table 8) and cloned into the yeast shuttle vector pWV3 between the *Bam*HI/*Xho*I and *Xho*I/*Eco*RI sites, respectively. Subsequently, the *AMT2;3* and *AMT2;4* fragments were released by *Bam*HI/*Xho*I and *Xho*I/*Eco*RI digestion respectively, blunt-ended by Klenow fill in, and subsequently ligated to the *Bam*HI linearized and blunt-ended yeast plasmid pYEUra3. The sequences of the coding regions were verified.

The vectors were then transformed into the yeast high-affinity ammonium transporter triple mutant (strain 31019b; ΔΔΔmep1;2;3) (Marini et al., 1997; kindly provide by Nuria Ferrol, CSIC, Spain). Yeast transformants were selected, and single colonies were grown in liquid YNB medium containing 3% galactose for 2 d. A positive control strain, ΔΔΔmep1;2;3::pFL61-GintAMT1 (López-Pedrosa et al., 2006) (kindly provided by Nuria Ferrol, CSIC, Spain), was grown in YNB containing 2% glucose. The cells were harvested, washed, and diluted to an OD_{600} of 0.2. Cell suspensions were spotted in 1- to 4-fold dilutions on YNB medium lacking amino acids at pH 4.5, supplemented with 5, 2, or 0.5 mM $(NH_4)_2SO_4$ as the sole nitrogen source and containing either glucose or galactose as a carbon source. The cells were then grown at 28°C for up to 6 d.

Generation and Analysis of *GFP-AMT2;3* and *GFP-AMT2;4* in Yeast

To create N-terminal GFP fusions for expression in yeast, the coding regions of *AMT2;3* and *AMT2;4* were amplified with the corresponding primers (Supplemental Table 8) and cloned into the CAMV35S-SGFP

(S65T)-Nos plasmid between the *Bsr*GI/*Not*I sites (Chiu et al., 1996). To release the GFP fusions, plasmids carrying GFP-*AMT2;3* and GFP-*AMT2;4* were digested with *Sal*I/*Xho*I and *Bam*HI/*Sal*I, respectively, and subsequently ligated either to *Sal*I/*Xho*I- or *Bam*HI/*Sal*I-digested pYEUra3 plasmid to generate $GAL1_{pro}$-GFP-*MtAMT2;3* and $GAL1_{pro}$-GFP-*MtAMT2;4*, respectively. The constructs were introduced into the yeast high-affinity ammonium transporter triple mutant (strain 31019b; ΔΔΔmep1;2;3). Yeast transformants were selected and single colonies were grown to induce expression of the fusion proteins as described (Drew et al., 2008). Yeast cells were examined by confocal microscopy as described previously (Liu et al., 2008), and the emission spectra of the cells were evaluated by lambda scanning.

Phylogenetic Analysis

The approximately maximum likelihood phylogenetic trees were generated using the predicted full-length amino acid sequences of phosphate transporters or ammonium transporters (Supplemental Data Sets 1 and 2). Sequences were obtained from Phytozome10 (*Arabidopsis thaliana*, *Oryza sativa*, *Sorghum bicolor*, and *Glycine max*), Solgenomics (*Solanum lycopersicum*), Kazusa DNA Research Institute (*Lotus japonicus*), and JCVI (*M. truncatula*). Alignments were generated using Muscle v3.8.31 with default values (Supplemental Data Sets 1 and 2). FastTree version 2.1.15 was used with default values to generate the phylogenies using a neighbor joining method to create a starting tree and later refining the topology using maximum likelihood nearest-neighbor interchanges and minimum-evolution subtree-pruning-regrafting. Each branch division shows local support values with the Shimodaira-Hasegawa test (Price et al., 2010).

Accession Numbers

Sequence data from this article can be found in the GenBank/EMBL libraries under the following accession numbers: *PT6* (Medtr3g082700), *PT7* (Medtr1g074940), *PT8* (Medtr5g068140), *PT9* (Medtr4g083960), *PT10* (Medtr1g069930), *PT11* (Medtr1g069935), *PT12* (Medtr7g096870), *PT13* (Medtr7g096880), *AMT2;1* (Medtr7g069640), *AMT2;2* (Medtr8g095040), *AMT2;3* (Medtr8g074750), *AMT2;4* (Medtr7g115050), *AMT2;5* (Medtr1g036410), and *AMT2;6* (Medtr4g017820).

Supplemental Data

Supplemental Figure 1. *M. truncatula* Pi transporters of the PHT1 family.

Supplemental Figure 2. Localization of PT8 and symbiosis phenotype of *pt8-1*.

Supplemental Figure 3. *M. truncatula* Tnt1 lines with insertions in *PT4*, *PT8* and *AMT2;3* and *AMT2;4.*

Supplemental Figure 4. Arbuscule images and arbuscule population structure in a Pi transporter double mutant.

Supplemental Figure 5. Morphology of AM symbiosis in *amt2;3* during growth in varying nitrogen and phosphate regimes.

Supplemental Figure 6. Morphology of AM symbiosis in *pt4-2 amt2;3* and *pt4-5 amt2;3.*

Supplemental Figure 7. Arbuscule populations in *pt4-2 amt2;3* and *pt4-5 amt2;3* at 8 days post-contact with *G. intraradices.*

Supplemental Figure 8. Arbuscule populations in a *pt4-5 pt8-1 amt2;3* triple mutant.

Supplemental Figure 9. Arbuscule populations in a *pt4-5 amt2;4* double mutant.

Supplemental Figure 10. Analysis of yeast 31019b (Δmep1; Δmep2; Δmep3) mep cells expressing *AMT2;3* and *AMT2;4* from the GAL1 promoter.

Supplemental Table 1. Shoot fresh weight and P and N content of the *pt4-2 pt8-1* and *pt4-5 pt8-1* Pi transporter double mutants in high-N growth conditions.

Supplemental Table 2. Shoot fresh weight and P and N content and infection unit length of the *pt4-2 pt8-1* and *pt4-5 pt8-1* Pi transporter double mutants in low-N growth conditions.

Supplemental Table 3. Shoot fresh weight and P and N content of the *pt4-2 amt2;3* and *pt4-5 amt2;3* double mutants in high-N growth conditions.

Supplemental Table 4. Shoot fresh weight and P and N content of the *pt4-2 amt2;3* and *pt4-5 amt2;3* double mutants in low-N growth conditions.

Supplemental Table 5. Shoot fresh weight and P and N content of the *pt4-5 pt8-1 amt2;3* triple mutant in low-N growth conditions.

Supplemental Table 6. Shoot fresh weight and P and N content of the *pt4-5 pt8-1 amt2;3* triple mutant, a wild-type segregant, and R108 in high-N growth conditions.

Supplemental Table 7. Shoot fresh weight and N content of the *pt4-5 pt8-1 amt2;3* triple mutant, a wild-type segregant, and R108 in low-N growth conditions.

Supplemental Table 8. Primer sequences.

Supplemental Data Set 1. PHT1 family alignment file.

Supplemental Data Set 2. AMT2 family alignment file.

ACKNOWLEDGMENTS

Financial support for this project was provided by National Science Foundation Grant IOS-0842720. F.B.-S. was supported in part by a fellowship from the Swiss National Science Foundation (PBFRP3-124343). We thank P. Ratet (CNRS, France) for the *pt4-5* allele, N. Ferrol (Estación Experimental del Zaidín CSIC, Spain) for the yeast ammonium transporter mutant expressing Gint-AMT1, and Jeon Hong for assistance with generation of genetic resources. J.B.E. was supported by funds donated by Carolyn Sampson and subsequently by IOS-0842720. With the exception of *pt4-5*, the *M. truncatula* Tnt1 insertion mutant lines were obtained from The Samuel Roberts Noble Foundation and were created through research funded in part by a grant from the National Science Foundation (DBI-0703285).

AUTHOR CONTRIBUTIONS

F.B.-S., N.P., S.K.G., D.S.F., Y.D., A.B., and M.J.H. designed research, performed research, analyzed data, and contributed to the writing of the article. V.L.-T., D.A.D., R.D.N., and J.B.E. performed research and analyzed data. V.A.B. and M.K.U. identified and contributed genetic resources.

Received August 21, 2014; revised February 22, 2015; accepted March 6, 2015; published April 3, 2015.

REFERENCES

Alexander, T., Meier, R., Toth, R., and Weber, H.C. (1988). Dynamics of arbuscule development and degeneration in mycorrhizas of *Triticum aestivum* L. and *Avena sativa* L. with reference to *Zea mays* L. New Phytol. **110:** 363–370.

Alexander, T., Toth, R., Meier, R., and Weber, H.C. (1989). Dynamics of arbuscule development and degeneration in onion, bean and tomato with reference to vesicular-arbuscular mycorrhizae in grasses. Can. J. Bot. **67:** 2505–2513.

Ames, B.N. (1966). Assay of inorganic phosphate, total phosphate and phosphatases. Methods Enzymol. **8:** 115–118.

Blanke, V., Renker, C., Wagner, M., Füllner, K., Held, M., Kuhn, A.J., and Buscot, F. (2005). Nitrogen supply affects arbuscular mycorrhizal colonization of *Artemisia vulgaris* in a phosphate-polluted field site. New Phytol. **166:** 981–992.

Boisson-Dernier, A., Chabaud, M., Garcia, F., Bécard, G., Rosenberg, C., and Barker, D.G. (2001). *Agrobacterium rhizogenes*-transformed roots of *Medicago truncatula* for the study of nitrogen-fixing and endomycorrhizal symbiotic associations. Mol. Plant Microbe Interact. **14:** 695–700.

Breuillin, F., et al. (2010). Phosphate systemically inhibits development of arbuscular mycorrhiza in *Petunia hybrida* and represses genes involved in mycorrhizal functioning. Plant J. **64:** 1002–1017.

Chiou, T.J., Liu, H., and Harrison, M.J. (2001). The spatial expression patterns of a phosphate transporter (MtPT1) from *Medicago truncatula* indicate a role in phosphate transport at the root/soil interface. Plant J. **25:** 281–293.

Chiu, W., Niwa, Y., Zeng, W., Hirano, T., Kobayashi, H., and Sheen, J. (1996). Engineered GFP as a vital reporter in plants. Curr. Biol. **6:** 325–330.

Cox, G., Moran, K.J., Sanders, F., Nockolds, C., and Tinker, P.B. (1980). Translocation and transfer of nutrients in vesicular-arbuscular mycorrhizas. III. Polyphosphate granules and phosphorus translocation. New Phytol. **84:** 649–659.

Crawford, N.M. (1995). Nitrate: nutrient and signal for plant growth. Plant Cell **7:** 859–868.

Cruz, C., Egsgaard, H., Trujillo, C., Ambus, P., Requena, N., Martins-Loução, M.A., and Jakobsen, I. (2007). Enzymatic evidence for the key role of arginine in nitrogen translocation by arbuscular mycorrhizal fungi. Plant Physiol. **144:** 782–792.

Drew, D., Newstead, S., Sonoda, Y., Kim, H., von Heijne, G., and Iwata, S. (2008). GFP-based optimization scheme for the overexpression and purification of eukaryotic membrane proteins in *Saccharomyces cerevisiae*. Nat. Protoc. **3:** 784–798.

Durr, M., Urech, K., Boller, T., Wiemken, A., Schwencke, J., and Nagy, M. (1979). Sequestration of arginine by polyphosphate in vacuoles of yeast (*Saccharomyces cerevisiae*). Arch. Microbiol. **121:** 169–175.

Ezawa, T., Smith, S.E., and Smith, F.A. (2001). Differentiation of polyphosphate metabolism between the extra- and intraradical hyphae of arbuscular mycorrhizal fungi. New Phytol. **149:** 555–563.

Fellbaum, C.R., Gachomo, E.W., Beesetty, Y., Choudhari, S., Strahan, G.D., Pfeffer, P.E., Kiers, E.T., and Bücking, H. (2012). Carbon availability triggers fungal nitrogen uptake and transport in arbuscular mycorrhizal symbiosis. Proc. Natl. Acad. Sci. USA **109:** 2666–2671.

Floss, D.S., Levy, J.G., Levesque-Tremblay, V., Pumplin, N., and Harrison, M.J. (2013). DELLA proteins regulate arbuscule formation in arbuscular mycorrhizal symbiosis. Proc. Natl. Acad. Sci. USA **110:** E2025–E5034.

Giots, F., Donaton, M.C.V., and Thevelein, J.M. (2003). Inorganic phosphate is sensed by specific phosphate carriers and acts in concert with glucose as a nutrient signal for activation of the protein kinase A pathway in the yeast *Saccharomyces cerevisiae*. Mol. Microbiol. **47:** 1163–1181.

Gomez, S.K., Javot, H., Deewatthanawong, P., Torres-Jerez, I., Tang, Y., Blancaflor, E.B., Udvardi, M.K., and Harrison, M.J. (2009). *Medicago truncatula* and *Glomus intraradices* gene expression in cortical cells harboring arbuscules in the arbuscular mycorrhizal symbiosis. BMC Plant Biol. **9:** 10.

Govindarajulu, M., Pfeffer, P.E., Jin, H., Abubaker, J., Douds, D.D., Allen, J.W., Bücking, H., Lammers, P.J., and Shachar-Hill, Y. (2005). Nitrogen transfer in the arbuscular mycorrhizal symbiosis. Nature **435:** 819–823.

Grunwald, U., Guo, W., Fischer, K., Isayenkov, S., Ludwig-Müller, J., Hause, B., Yan, X., Küster, H., and Franken, P. (2009). Overlapping expression patterns and differential transcript levels of phosphate transporter genes in arbuscular mycorrhizal, Pi-fertilised and phytohormone-treated *Medicago truncatula* roots. Planta **229:** 1023–1034.

Guether, M., Neuhäuser, B., Balestrini, R., Dynowski, M., Ludewig, U., and Bonfante, P. (2009). A mycorrhizal-specific ammonium transporter from Lotus japonicus acquires nitrogen released by arbuscular mycorrhizal fungi. Plant Physiol. **150:** 73–83.

Hammer, E.C., Pallon, J., Wallander, H., and Olsson, P.A. (2011). Tit for tat? A mycorrhizal fungus accumulates phosphorus under low plant carbon availability. FEMS Microbiol. Ecol. **76:** 236–244.

Harrison, M.J. (2012). Cellular programs for arbuscular mycorrhizal symbiosis. Curr. Opin. Plant Biol. **15:** 691–698.

Harrison, M.J., Dewbre, G.R., and Liu, J. (2002). A phosphate transporter from *Medicago truncatula* involved in the acquisition of phosphate released by arbuscular mycorrhizal fungi. Plant Cell **14:** 2413–2429.

Harrison, M.J., Pumplin, N., Breuillin, F.J., Noar, R.D., and Park, H.-J. (2010). Phosphate transporters in arbuscular mycorrhizal symbiosis. In Arbuscular Mycorrhizas: Physiology and Function, H. Koltai, and Y. Kapulnik, eds (New York: Springer), pp. 117–137.

Hijikata, N., Murase, M., Tani, C., Ohtomo, R., Osaki, M., and Ezawa, T. (2010). Polyphosphate has a central role in the rapid and massive accumulation of phosphorus in extraradical mycelium of an arbuscular mycorrhizal fungus. New Phytol. **186:** 285–289.

Hodge, A., and Fitter, A.H. (2010). Substantial nitrogen acquisition by arbuscular mycorrhizal fungi from organic material has implications for N cycling. Proc. Natl. Acad. Sci. USA **107:** 13754–13759.

Hodge, A., Campbell, C.D., and Fitter, A.H. (2001). An arbuscular mycorrhizal fungus accelerates decomposition and acquires nitrogen directly from organic material. Nature **413:** 297–299.

Hong, J.J., Park, Y.S., Bravo, A., Bhattarai, K.K., Daniels, D.A., and Harrison, M.J. (2012). Diversity of morphology and function in arbuscular mycorrhizal symbioses in *Brachypodium distachyon*. Planta **236:** 851–865.

Javot, H., Penmetsa, R.V., Terzaghi, N., Cook, D.R., and Harrison, M.J. (2007). A *Medicago truncatula* phosphate transporter indispensable for the arbuscular mycorrhizal symbiosis. Proc. Natl. Acad. Sci. USA **104:** 1720–1725.

Javot, H., Penmetsa, R.V., Breuillin, F., Bhattarai, K.K., Noar, R.D., Gomez, S.K., Zhang, Q., Cook, D.R., and Harrison, M.J. (2011). *Medicago truncatula mtpt4* mutants reveal a role for nitrogen in the regulation of arbuscule degeneration in arbuscular mycorrhizal symbiosis. Plant J. **68:** 954–965.

Johansen, A., Jakobsen, I., and Jensen, E.S. (1993). External hyphae of vesicular-arbuscular mycorrhizal fungi associated with *Trifolium subterraneum* L. 3. Hyphal transport of P-32 and N-15. New Phytol. **124:** 61–68.

Johnson, N.C., Wilson, G.W.T., Bowker, M.A., Wilson, J.A., and Miller, R.M. (2010). Resource limitation is a driver of local adaptation in mycorrhizal symbioses. Proc. Natl. Acad. Sci. USA **107:** 2093–2098.

Kant, S., Peng, M., and Rothstein, S.J. (2011). Genetic regulation by NLA and microRNA827 for maintaining nitrate-dependent phosphate homeostasis in arabidopsis. PLoS Genet. **7:** e1002021.

Karandashov, V., and Bucher, M. (2005). Symbiotic phosphate transport in arbuscular mycorrhizas. Trends Plant Sci. **10:** 22–29.

Kiers, E.T., et al. (2011). Reciprocal rewards stabilize cooperation in the mycorrhizal symbiosis. Science **333:** 880–882.

Kobae, Y., and Hata, S. (2010). Dynamics of periarbuscular membranes visualized with a fluorescent phosphate transporter in arbuscular mycorrhizal roots of rice. Plant Cell Physiol. **51:** 341–353.

Kobae, Y., Tamura, Y., Takai, S., Banba, M., and Hata, S. (2010). Localized expression of arbuscular mycorrhiza-inducible ammonium transporters in soybean. Plant Cell Physiol. **51:** 1411–1415.

Koegel, S., Ait Lahmidi, N., Arnould, C., Chatagnier, O., Walder, F., Ineichen, K., Boller, T., Wipf, D., Wiemken, A., and Courty, P.-E. (2013). The family of ammonium transporters (AMT) in *Sorghum bicolor*:

two AMT members are induced locally, but not systemically in roots colonized by arbuscular mycorrhizal fungi. New Phytol. **198:** 853–865.

Koide, R.T., and Li, M.G. (1990). On host regulation of the vesicular arbuscular mycorrhizal symbiosis. New Phytol. **114:** 59–64.

Koide, R.T., and Schreiner, R.P. (1992). Regulation of the vesicular-arbuscular mycorrhizal symbiosis. Annu. Rev. Plant Physiol. Plant Mol. Biol. **43:** 557–581.

Kretzschmar, T., Kohlen, W., Sasse, J., Borghi, L., Schlegel, M., Bachelier, J.B., Reinhardt, D., Bours, R., Bouwmeester, H.J., and Martinoia, E. (2012). A petunia ABC protein controls strigolactone-dependent symbiotic signalling and branching. Nature **483:** 341–344.

Krouk, G., Mirowski, P., LeCun, Y., Shasha, D.E., and Coruzzi, G.M. (2010). Predictive network modeling of the high-resolution dynamic plant transcriptome in response to nitrate. Genome Biol. **11:** R123.

Lanfranco, L., and Young, J.P.W. (2012). Genetic and genomic glimpses of the elusive arbuscular mycorrhizal fungi. Curr. Opin. Plant Biol. **15:** 454–461.

Leigh, J., Hodge, A., and Fitter, A.H. (2009). Arbuscular mycorrhizal fungi can transfer substantial amounts of nitrogen to their host plant from organic material. New Phytol. **181:** 199–207.

Lima, J.E., Kojima, S., Takahashi, H., and von Wirén, N. (2010). Ammonium triggers lateral root branching in Arabidopsis in an AMMONIUM TRANSPORTER1;3-dependent manner. Plant Cell **22:** 3621–3633.

Liu, H., Trieu, A.T., Blaylock, L.A., and Harrison, M.J. (1998). Cloning and characterization of two phosphate transporters from *Medicago truncatula* roots: regulation in response to phosphate and to colonization by arbuscular mycorrhizal (AM) fungi. Mol. Plant Microbe Interact. **11:** 14–22.

Liu, J., Versaw, W.K., Pumplin, N., Gomez, S.K., Blaylock, L.A., and Harrison, M.J. (2008). Closely related members of the *Medicago truncatula* PHT1 phosphate transporter gene family encode phosphate transporters with distinct biochemical activities. J. Biol. Chem. **283:** 24673–24681.

Lopez-Meyer, M., and Harrison, M.J. (2006). An experimental system to synchronize the early events of development of the arbuscular mycorrhizal symbiosis. In Biology of Molecular Plant-Microbe Interactions, F. Sánchez, C. Quinto, I.M. López-Lara, and O. Geiger, eds (St Paul, MN: International Society for Molecular Plant Microbe Interactions), pp. 546–551.

López-Pedrosa, A., González-Guerrero, M., Valderas, A., Azcón-Aguilar, C., and Ferrol, N. (2006). GintAMT1 encodes a functional high-affinity ammonium transporter that is expressed in the extraradical mycelium of *Glomus intraradices*. Fungal Genet. Biol. **43:** 102–110.

Marini, A.M., Soussi-Boudekou, S., Vissers, S., and Andre, B. (1997). A family of ammonium transporters in *Saccharomyces cerevisiae*. Mol. Cell. Biol. **17:** 4282–4293.

Martinez, P., and Persson, B.L. (1998). Identification, cloning and characterization of a derepressible Na^+-coupled phosphate transporter in *Saccharomyces cerevisiae*. Mol. Gen. Genet. **258:** 628–638.

McGonigle, T.P., Miller, M.H., Evans, D.G., Fairchild, G.L., and Swan, J.A. (1990). A new method that gives an objective measure of colonization of roots by vesicular-arbuscular mycorrhizal fungi. New Phytol. **115:** 495–501.

Morcuende, R., Bari, R., Gibon, Y., Zheng, W., Pant, B.D., Bläsing, O., Usadel, B., Czechowski, T., Udvardi, M.K., Stitt, M., and Scheible, W.R. (2007). Genome-wide reprogramming of metabolism and regulatory networks of Arabidopsis in response to phosphorus. Plant Cell Environ. **30:** 85–112.

Paszkowski, U., Kroken, S., Roux, C., and Briggs, S.P. (2002). Rice phosphate transporters include an evolutionarily divergent gene specifically activated in arbuscular mycorrhizal symbiosis. Proc. Natl. Acad. Sci. USA **99:** 13324–13329.

Pérez-Tienda, J., Corrêa, A., Azcón-Aguilar, C., and Ferrol, N. (2014). Transcriptional regulation of host NH_4^+ transporters and GS/GOGAT pathway in arbuscular mycorrhizal rice roots. Plant Physiol. Biochem. **75:** 1–8.

Price, M.N., Dehal, P.S., and Arkin, A.P. (2010). FastTree 2—approximately maximum-likelihood trees for large alignments. PLoS ONE **5:** e9490.

Pumplin, N., Mondo, S.J., Topp, S., Starker, C.G., Gantt, J.S., and Harrison, M.J. (2010). Medicago truncatula Vapyrin is a novel protein required for arbuscular mycorrhizal symbiosis. Plant J. **61:** 482–494.

Qin, L., Guo, Y., Chen, L., Liang, R., Gu, M., Xu, G., Zhao, J., Walk, T., and Liao, H. (2012). Functional characterization of 14 Pht1 family genes in yeast and their expressions in response to nutrient starvation in soybean. PLoS ONE **7:** e47726.

Rubio-Texeira, M., Van Zeebroeck, G., Voordeckers, K., and Thevelein, J.M. (2010). *Saccharomyces cerevisiae* plasma membrane nutrient sensors and their role in PKA signaling. FEMS Yeast Res. **10:** 134–149.

Ruzicka, D.R., Hausmann, N.T., Barrios-Masias, F.H., Jackson, L.E., and Schachtman, D.P. (2012). Transcriptomic and metabolic responses of mycorrhizal roots to nitrogen patches under field conditions. Plant Soil **350:** 145–162.

Sanders, F.E., and Tinker, P.B. (1971). Mechanism of absorption of phosphate from soil by *Endogone* mycorrhizas. Nature **233:** 278–279.

Scheible, W.R., Morcuende, R., Czechowski, T., Fritz, C., Osuna, D., Palacios-Rojas, N., Schindelasch, D., Thimm, O., Udvardi, M.K., and Stitt, M. (2004). Genome-wide reprogramming of primary and secondary metabolism, protein synthesis, cellular growth processes, and the regulatory infrastructure of Arabidopsis in response to nitrogen. Plant Physiol. **136:** 2483–2499.

Smith, S.E., and Read, D.J. (2008). Mycorrhizal Symbiosis. (San Diego, CA: Academic Press).

Smith, S.E., and Smith, F.A. (2011). Roles of arbuscular mycorrhizas in plant nutrition and growth: New paradigms from cellular to ecosystem scales. Annu. Rev. Plant Biol. **62:** 227–250.

Stitt, M. (1999). Nitrate regulation of metabolism and growth. Curr. Opin. Plant Biol. **2:** 178–186.

Straub, D., Ludewig, U., and Neuhäuser, B. (2014). A nitrogen-dependent switch in the high affinity ammonium transport in *Medicago truncatula*. Plant Mol. Biol. **86:** 485–494.

Tamura, Y., Kobae, Y., Mizuno, T., and Hata, S. (2012). Identification and expression analysis of arbuscular mycorrhiza-inducible phosphate transporter genes of soybean. Biosci. Biotechnol. Biochem. **76:** 309–313.

Tanaka, Y., and Yano, K. (2005). Nitrogen delivery to maize via mycorrhizal hyphae depends on the form of N supplied. Plant Cell Environ. **28:** 1247–1254.

Van Nuland, A., Vandormael, P., Donaton, M., Alenquer, M., Lourenço, A., Quintino, E., Versele, M., and Thevelein, J.M. (2006). Ammonium permease-based sensing mechanism for rapid ammonium activation of the protein kinase A pathway in yeast. Mol. Microbiol. **59:** 1485–1505.

Versaw, W.K., and Harrison, M.J. (2002). A chloroplast phosphate transporter, PHT2;1, influences allocation of phosphate within the plant and phosphate-starvation responses. Plant Cell **14:** 1751–1766.

Xiao, K., Liu, J., Dewbre, G., Harrison, M., and Wang, Z.-Y. (2006). Isolation and characterization of root-specific phosphate transporter promoters from *Medicago truncatula*. Plant Biol. (Stuttg.) **8:** 439–449.

Xie, X., Huang, W., Liu, F., Tang, N., Liu, Y., Lin, H., and Zhao, B. (2013). Functional analysis of the novel mycorrhiza-specific phosphate transporter AsPT1 and PHT1 family from *Astragalus sinicus* during the arbuscular mycorrhizal symbiosis. New Phytol. **198:** 836–852.

Yang, S.Y., and Paszkowski, U. (2011). Phosphate import at the arbuscule: just a nutrient? Mol. Plant Microbe Interact. **24:** 1296–1299.

Yang, S.Y., et al. (2012). Nonredundant regulation of rice arbuscular mycorrhizal symbiosis by two members of the phosphate transporter1 gene family. Plant Cell **24:** 4236–4251.

Yoneyama, K., Xie, X., Kim, H.I., Kisugi, T., Nomura, T., Sekimoto, H., Yokota, T., and Yoneyama, K. (2012). How do nitrogen and phosphorus deficiencies affect strigolactone production and exudation? Planta **235:** 1197–1207.